Synthesis, Characterization, and Cytotoxic Assessment of Novel S-Naproxen-based 1,3,4-Oxadiazole Thioethers against A549 Lung Carcinoma

Farooq Mohammed Hassan*, Ayad Kareem Khan*, Shakir Mahmood Alwan, Mohammad M. Al-Akaidi*****

Department of Pharmaceutical Chemistry, College of Pharmacy, Mustansiriyah University, Baghdad, Iraq

****College of Pharmacy, Alshaab University, Baghdad, Iraq.***

*****Clinical Teaching Fellow, University of Leicester, UK.***

Article Info:

Received 1 May 2025
Revised 1 July 2025
Accepted 4 Aug 2025
Published 31 Dec 2025
Corresponding Author email:
farooqalgaragoolee22@uomustansiriyah.edu.iq
Orcid: https://orcid.org/0009-0005-3998-3248

DOI: https://doi.org/10.32947/ajps.v25i5.1320

Abstract:

Novel S-naproxen- 1,3,4-oxadiazole derivatives were developed and synthesized via a multi-step route. The synthesis began with conversion of S-(+)-naproxen to an ethyl ester, followed by hydrazide formation and cyclization to yield a 1,3,4-oxadiazole-2-thiol intermediate. Alkylation of this intermediate with various substituted phenacyl bromides produced nine final 1,3,4-oxadiazole thioether derivatives (N1–N9).

The structures of all compounds were confirmed by Fourier-transform infrared (FT-IR) spectroscopy, and nuclear magnetic resonance (NMR) (^{1}H and ^{13}C-NMR) analysis. Preliminary in vitro cytotoxicity was evaluated against human lung adenocarcinoma A549 cells using the MTT assay. All compounds demonstrated growth inhibition, with IC_{50} values in the low microgram per milliliter range. Notably, compound N6 showed an IC_{50} of 2.94 µg/mL at 24 h (versus 5.31 µg/mL for the reference drug Osimertinib). After 72 h exposure, the most potent derivative, N9, achieved an IC_{50} of 2.95 µg/mL, slightly surpassing Osimertinib (3.10 µg/mL) . These findings indicate that S-naproxen 1,3,4-oxadiazole thioethers are promising anticancer agents. The incorporation of the 2-(6-methoxynaphthyl) (naproxen) moiety and various aromatic substituents yielded compounds with potent antiproliferative activity, warranting further development and in-depth biological studies.

Keywords: 1,3,4-Oxadiazole, Naproxen, Lung cancer, Synthesis, Cytotoxic activity.

تحضير وتوصيف وتقييم السمية الخلوية لمشتقات ثيوإيثر جديدة قائمة على أس-نابروكسين من نوع 1,3,4-أوكساديازول ضد خلايا سرطان الرئة A549

فاروق محمد حسن *, اياد كريم خان *, شاكر محمود علوان **, محمد العقيدي***

قسم الكيمياء الصيدلانية، كلية الصيدلة، الجامعة المستنصرية، بغداد، العراق.

****كلية الصيدلة، جامعة الشعب، بغداد، العراق.***

*****اكاديمي سريري، جامعة ليستر، إنكلترا.***

الخلاصة:

تم تطوير وتحضير مشتقات جديدة من ثيوإيثر أوكساديازول 1,3,4 المشتقة من أس-نابروكسين من خلال مسار متعدد الخطوات. بدأت عملية التحضير بتحويل أس-(+) -نابروكسين إلى الإستر الإيثيلي، تلاه تكوين الهيدرازيد ثم الحلقنة لإنتاج مركب وسيط من أوكساديازول-2-ثيول. تم إجراء تفاعل ألكلة لهذا الوسيط باستخدام مجموعة متنوعة من بروميدات

الفيناكزيل المستبدلة لإنتاج تسع مشتقات نهائية من ثيوإيثر أوكساديازول 1,3,4 .(N1–N9) تم تأكيد تراكيب جميع المركبات بواسطة درجة الانصهار، مطيافية الأشعة تحت الحمراء(FT-IR) ، وتحاليل الرنين المغناطيسي النووي ^{1}H) و-^{13}C NMR).
تم تقييم السمية الخلوية الأولية للمركبات في المختبر ضد خلايا سرطان الرئة الغدية البشرية A549 باستخدام اختبار السمية الخلوية .أظهرت جميع المركبات قدرة ملحوظة على تثبيط النمو، مع قيم IC_{50} ضمن نطاق الميكروغرام/مل. برز المركب N6بقيمة IC_{50} بلغت 2.94 ميكروغرام/مل بعد 24 ساعة مقارنةً بـ 5.31 ميكروغرام/مل لدواء أوسيميرتينيب المرجعي. بعد 72 ساعة من التعرض، كان المركب N9 هو الأكثر فاعلية، حيث حقق IC_{50} بمقدار 2.95 ميكروغرام/مل، متفوقًا قليلًا على أوسيميرتينيب (3.10 ميكروغرام/مل).
تشير هذه النتائج إلى أن مشتقات ثيوإيثر أوكساديازول 1,3,4 المشتقة من أس-نابروكسين تُعد عوامل واعدة مضادة للسرطان. وقد أدى دمج مجموعة 2-(6-ميثوكسي نفثيل) (نابروكسين) مع مستبدلات عطرية متنوعة إلى الحصول على مركبات ذات نشاط مثبط قوي للتكاثر، مما يستدعي مزيدًا من التطوير والدراسات البيولوجية المتعمقة.

الكلمات المفتاحية :أوكساديازول 1,3,4، نابروكسين، سرطان الرئة، تحضير، النشاط السمي الخلوي.

Introduction

Lung cancer is a prevalent malignancy and the primary cause of cancer-related deaths globally. Non-small cell lung cancer (NSCLC) constitutes the predominant majority of cases. Notwithstanding progress in treatment, including molecularly targeted therapies, lung cancer survival rates continue to be unacceptably poor [1]. Targeting dysregulated signaling pathways, such as the epidermal growth factor receptor (EGFR), has demonstrated efficacy in the treatment of non-small cell lung cancer (NSCLC). Numerous small-molecule EGFR tyrosine kinase inhibitors (TKIs) are utilized in clinical practice; for instance, Osimertinib is a third-generation EGFR-TKI developed to address the T790M resistance mutation in non-small cell lung cancer (NSCLC). The rise of drug resistance and off-target consequences necessitates the ongoing pursuit of novel anticancer scaffolds and inhibitors [1].

Heterocyclic compounds bearing the 1,3,4-oxadiazole ring have attracted considerable interest in medicinal chemistry due to their diverse biological activities, including anticancer effects. The 1,3,4-oxadiazole nucleus is a five-membered ring containing two nitrogen and one oxygen heteroatoms, which confer desirable pharmacological properties and drug-like characteristics [2] . Numerous 1,3,4-oxadiazole derivatives have shown promising antiproliferative activity in vitro and in vivo, often by interfering with receptor tyrosine kinase (RTK) signaling pathways [2] . Indeed, recent studies have reported 1,3,4-oxadiazoles as potent inhibitors of oncogenic kinases such as vascular endothelial growth factor receptor (VEGFR) and EGFR [3] . A comprehensive literature review revealed that 1,3,4-oxadiazole-based compounds frequently exhibit significant anticancer efficacy , validating this heterocycle as a privileged scaffold in cancer drug design [4].

Another important motif in cancer chemoprevention is the 2-(6-methoxynaphthalen-2-yl) propionic acid backbone, commonly known as naproxen [5]. Naproxen is a well-known nonsteroidal anti-inflammatory drug (NSAID) that has been safely used for decades for pain and inflammation. In recent years, beyond its cyclooxygenase (COX) inhibitory activity, naproxen itself and its derivatives have demonstrated noteworthy antiproliferative and anticancer properties [6] . The anticancer effects of naproxen are thought to be related to COX-2 inhibition and possibly COX-independent mechanisms, prompting efforts to repurpose or modify this scaffold for oncology applications . Prior studies have explored naproxen derivatives incorporating various heterocycles to enhance biological activity. For example, researchers, [2] designed a hybrid molecule linking an S-naproxen fragment with 1,3,4-oxadiazole and 1,2,3-triazole moieties; this compound was equipotent to doxorubicin against HepG2

hepatocellular carcinoma cells and notably inhibited EGFR kinase with a good activity comparable to the standard EGFR inhibitor erlotinib. This finding highlights the potential of combining the 6-methoxynaphthalene (naproxen) pharmacophore with a 1,3,4-oxadiazole ring to yield effective kinase inhibitors. In another report, [7] A series of naphthalene-oxadiazole thioethers derivatives were synthesized that showed potent cytotoxicity against breast and liver cancer cell lines and significant activity against VEGFR-2 in vitro. These studies provide a strong rationale for merging the naproxen scaffold with a 1,3,4-oxadiazole heterocycle to develop new anticancer agents targeting aberrant signaling pathways in cancer cells. In light of the above, our objective was to design and synthesize a variety of new S-naproxen-derived 1,3,4-oxadiazole derivatives and assess their cytotoxic efficacy against lung cancer cells. This study details the chemical synthesis of nine novel 1,3,4-oxadiazol-2-yl thioether derivatives of S-naproxen (designated N1–N9), each incorporating different para-substituted phenyl groups on the thioether bond. The molecules were synthesized by a four-step process (Scheme 1) commencing with naproxen.

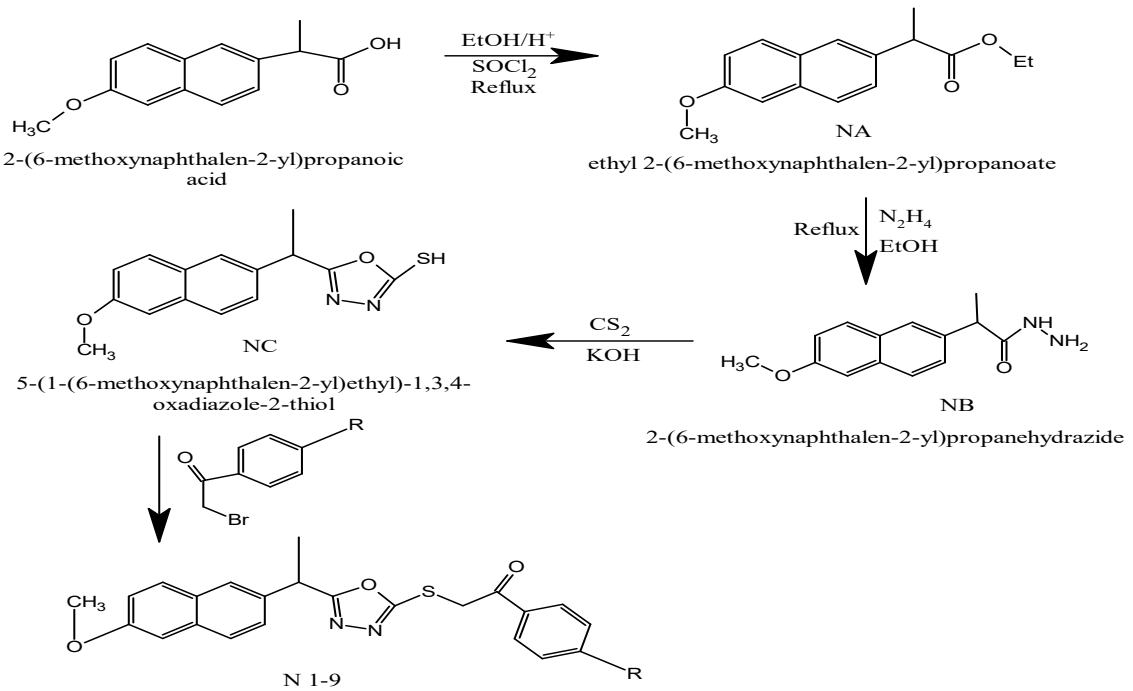

R= 4-**Cl (N8)**, 4-**Br (N9)**, 4-**H (N3)**, 4-**NH_2 (N1)**, 4-**CH_3 (N4)**, 4-**$N(CH_3)_2$ (N2)**, 4-**OH (N7)**, 4-**NO_2 (N6)**, 4-**CH_2CH_3 (N5)**

Scheme (1): Synthesis of the intermediate and final compounds.

Materials and Methods

Chemicals and Instrumentation

S-(+)-Naproxen (purity 99%) was obtained from HyperChem (China) and used as the starting material. Thionyl chloride, hydrazine hydrate (99%), carbon disulfide, potassium hydroxide, phenacyl bromides (para-substituted acetophenone bromides), and all other reagents and solvents were purchased from commercial suppliers (Thomas Baker, Alpha Chemika, etc.)

Reactions were monitored via thin-layer chromatography (TLC) on silica gel plates with suitable solvent systems (e.g., hexane/ethyl acetate). Melting points were determined using a Stuart digital melting point equipment (UK). FT-IR spectra were obtained using a Shimadzu 8400S FT-IR spectrophotometer (Japan) with KBr

pellets, over the range of 4000–400 cm^{-1}. Nuclear magnetic resonance spectra (^{1}H-NMR and ^{13}C-NMR) were obtained using Bruker H-NMR spectrometers operating at *400* MHz for ^{1}H-NMR and *75* MHz for ^{13}C-NMR, employing deuterated solvents (*DMSO-d6*) with tetramethyl silane (TMS) as an internal standard. The spectra were analyzed to verify the structures of the produced substances.

Synthesis of S-naproxen 1,3,4-oxadiazole Thioether Derivatives (N1–N9)

Step 1: Esterification of Naproxen (Compound NA). S-(+)-Naproxen (4.67 mmol, 1.0 g) was dissolved in 5 mL of absolute ethanol (in a fume hood), thionyl chloride (0.32 ml, 4.5mmol), and concentrated H_2SO_4 (0.3 mL) was added dropwise with stirring. The reaction mixture was refluxed for ~5 hours, then stirred at room temperature overnight. After completion, the mixture was poured into ice-water and neutralized with saturated $NaHCO_3$. The precipitate was extracted with ethyl acetate; the organic layer was washed with brine and dried over Na_2SO_4. Solvent removal and recrystallization from hexane afforded the ethyl ester (NA) as white crystals [8].

Step 2: Hydrazide formation (Compound NB). The ester NA (1.0 mmol) was dissolved in 15 mL of absolute ethanol in a 100 mL round-bottom flask. Hydrazine hydrate (99%, 5 mmol, 0.25 ml) was added, and the mixture was refluxed for 8–11 hours. After cooling to room temperature, the reaction mixture was poured into ice-water, inducing precipitation of the product. The solid was filtered, washed with cold water then recrystallized in ethanol, and dried to yield the acid hydrazide (NB) as an off-white fluffy powder [9].

Step 3: Cyclization to 1,3,4-oxadiazole-2-thiol (Compound NC). The hydrazide NB (5 mmol,0.5 ml) was dissolved in ethanol (30 mL) and potassium hydroxide (5 mmol,0.28 g) was added. The mixture was heated to 60 °C for 15 minutes, then carbon disulfide (5 mmol, 0.5ml) was added dropwise. The reaction was refluxed under stirring for 6 hours, during which the progress was monitored by TLC (hexane: ethyl acetate 6:4). After completion, the hot mixture was poured onto crushed ice. A white precipitate formed immediately, which was filtered, washed with water, and air-dried to give the cyclized oxadiazole-2-thiol (NC). The crude product was recrystallized from ethanol for further purification [10].

Step 4: S-Alkylation to final thioether derivatives (Compounds N1–N9). A series of phenacyl bromide derivatives (0.5 mmol) bearing different para-substituents (R = $4NH_2$, $4N(CH_3)_2$, H, 4-CH_3, 4-C $_2H_5$, 4-NO_2, 4-OH, 4-Cl, 4-Br) were used to alkylate the thiol NC. In a typical reaction, the oxadiazole-2-thiol NC (0.5 mmol, 0.14 g) and triethylamine (0.5 mmol, 0.07 mL) were dissolved in ethanol (10 mL) in a 100 mL flask. To this solution, the appropriate phenacyl bromide (0.5 mmol) was added in drop wise. The mixture was refluxed for 3–5 hours. TLC was performed (hexane: ethyl acetate 6:4) to monitor the consumption of starting material. After completion, the reaction mixture was poured into ice-water. The resulting precipitate was collected by filtration, washed with cold water and then with hexane, and vacuum-dried to yield the final products N1–N9 [11]. Each crude product was recrystallized from ethanol to afford the target compound in pure form. The structures of the nine final compounds are shown in (scheme 1).

Cytotoxicity Evaluation (MTT Assay)

Cellular lines and cultivation. The A549 lung cancer cell line was acquired from the National Cell Bank of Iran (Pasteur Institute, Iran). Cells were cultured in RPMI-1640 media (Gibco) with 10% FBS (Gibco) and treated with antibiotics (100 U/ml penicillin and 100 µg/ml

streptomycin). Cells were cultured at 37 °C in humidified air with 5% CO_2 and were subculture using trypsin/EDTA (Gibco) and phosphate-buffered saline (PBS) solution [12].

Data Analysis: Cell viability in treated wells was expressed as a percentage of the untreated control wells (cells with no drug, considered 100% viable). The growth inhibition (%) for each drug concentration was calculated as 100 minus the percent viability. **IC_{50}** values (the concentration of compound required to inhibit cell growth by 50%) were determined from the dose–response curves. **IC_{50}** calculations were performed separately for 24 h, 48 h, and 72 h treatment durations for each compound, using nonlinear regression analysis in Origin Lab Pro software. Osimertinib (a known EGFR-targeting drug for NSCLC) was included as a positive control in the assay for comparison. All experiments were carried out in duplicate or triplicate, and the average values are reported.

Results and Discussion

Chemical Synthesis and Characterization

The target S-naproxen oxadiazole derivatives (N1–N9) were successfully synthesized through a four-step sequence as outlined in Scheme 1. In the first step, naproxen was esterified to ethyl (S)-2-(6-methoxynaphthalen-2-yl) propanoate (NA) using acid-catalyzed condensation with ethanol. The formation of NA was confirmed, Yield: 95%; m.p. 92–94 °C (lit. 93 °C). (hexane: ethyl acetate 6:4). FT-IR (KBr) showed the disappearance of the C=O of carboxylic acid group of naproxen (originally at 1735 cm^{-1}) and the appearance of a strong new band at 1747 cm^{-1} corresponding to the ester carbonyl (–C=O) . The C–O stretching of the ester was evident at 1290 and 1227 cm^{-1}, and aromatic C–H stretches appeared around 3060 cm^{-1} [13]. These spectral changes confirmed successful formation of the naproxen ethyl ester (NA).

The melting point of NA (92–94 °C) was significantly lower than that of the parent acid naproxen (153–154 °C), consistent with its less rigid structure and absence of strong hydrogen bonding. These findings agree with literature data for naproxen esters.

In the second step, conversion of the ester to the corresponding hydrazide (NB) was achieved by refluxing with an excess of hydrazine hydrate. The reaction involves nucleophilic acyl substitution, in which hydrazine (NH_2NH_2) replaces the ethoxy group (–OEt), yielding the carboxylic hydrazide. After the reaction, the crude product was thoroughly purified by recrystallization from ethanol to eliminate any unreacted ester. Yield: 78%; m.p. 136–138 °C (lit. 137 °C). FT-IR (KBr) analysis of NB showed the disappearance of the ester carbonyl band at 1745 cm^{-1} and the appearance of a new amide carbonyl absorption at 1665 cm^{-1}. Additionally, N–H stretching vibrations at 3305, 3274, and 3210 cm^{-1} (from –$NHNH_2$) confirmed formation of the hydrazide. The absence of residual ester peaks in the purified sample confirmed the success of both the reaction and the purification step [1,2]. In third step, cyclization of the hydrazide (NB) with carbon disulfide in basic ethanol yielded the key heterocyclic intermediate, 5-(1-(6-methoxynaphthalen-2-yl) ethyl)-1,3,4-oxadiazole-2-thiol (NC). The reaction conditions (KOH in ethanol, CS_2, reflux) facilitated the formation of the 1,3,4-oxadiazole ring via a cyclo-condensation mechanism as shown in (scheme 2) . Mechanistically, the deprotonated hydrazide attacks carbon disulfide to form a dithiocarbazate intermediate, which then eliminates sulfide and cyclizes, releasing KHS (potassium hydrosulfide) and water to form the oxadiazole-2-thiol . The presence of a base (KOH) is crucial both for deprotonating the hydrazide (increasing nucleophilicity) and for facilitating ring closure (by removing H_2S or KHS). The

formation of the oxadiazole was evidenced by the IR spectrum: NB's amide C=O (1654 cm^{-1}) was disappeared, and new bands appeared at 1621 cm^{-1} (C=N) and 1120–1165 cm^{-1} (C–O–C and C–S stretches) . The product NC still contained a thiol (–SH) group, confirmed by a ^{1}H-NMR singlet at δ 13.32 ppm. The high de-shielding of this proton is typical for thiols adjacent to electron-withdrawing heterocycles (here, the oxadiazole ring and naphthalene). NC was obtained in 90% yield as a white solid, m.p. 192–194 °C (lit. 193 °C). Rf*:* 0.92. The ^{13}C-NMR spectrum of NC exhibited a signal at δ 166.5 ppm, corresponding to the C-5 of the oxadiazole ring. These spectroscopic features confirm the successful cyclization of NB to the 1,3,4-oxadiazole-2-thiol NC. indicating that the cyclization was efficient. This approach to 1,3,4-oxadiazole-2-thiol from acyl hydrazide and CS_2 is well documented in the literature [10] and provided a convenient entry to our target scaffold.

In the fourth step, the thiol NC was S-alkylated with various phenacyl bromides (para-substituted benzoyl methyl bromides) to furnish the desired thioether-linked oxadiazoles (N1–N9). The reaction is essentially an SN_2 nucleophilic substitution: the thiolate anion (generated by deprotonation of NC with triethylamine) attacks the methylene carbon of the phenacyl bromide, displacing bromide and forming a new C–S bond . We observed that the reaction went to completion within a few hours under reflux in ethanol, and the precipitation of products upon quenching into water facilitated isolation. The yields for this step were generally good (65–80%) across different substituents, suggesting that neither strong electron-withdrawing nor electron-donating groups on the phenacyl bromide had a severely detrimental effect on the coupling reaction. The mechanism is illustrated in Scheme 3, showing the thiolate SN_2 attack on the phenacyl carbon to give the thioether. All nine final compounds were characterized thoroughly. The disappearance of the –SH proton in the ^{1} H-NMR and the loss of the thiol IR band indicated successful thioether formation. Instead, each molecule exhibited signals corresponding to the new aryl substituent. For example, comparing NC vs. N8 (4-chlorophenyl derivative): NC had an –SH IR/NMR signal, whereas N8 showed an absence of –SH and new aromatic signals from the p-chlorophenyl group (C–Cl stretch 800 cm^{-1}, aromatic protons 7.2–7.8 ppm). The formation of thioethers was further supported by the presence of a methylene signal (–CH_2– linker between the phenyl and oxadiazole) around δ 4.5–5.0 ppm in ^{1}H-NMR for all N1–N9, which was absent in NC. Notably, the final compounds generally have high melting points (mostly >140 °C, except N4 which melts at 116–118 °C) and are solids ranging from white to yellow/brown depending on the substituent. This is expected given their aromatic, polyfunctional structures.

Characterization of Synthesized Compounds:

ethyl 2-(6-methoxynaphthalen-2-yl)propanoate (NA) - White crystal, yield = 95%, m.p. = 92-94 °C. FTIR (cm^{-1}): 3055 (Aromatic C-H), 2954, 2897 (CH_3, CH_2), 1747 (C=O, ester), 1448-1361 (CH_3, CH_2 bending), 1273, 1226 (C-O-C, methoxy), 1226 (C-O, ester), 813 (naphthalene ring out-of-plane bending), with formula: ($C_{16}H_{18}O_3$).

2-(6-methoxynaphthalen-2-yl)propane hydrazide (NB) - Off-white fluffy powder, yield = 78%, m.p. = 136-138 °C. FTIR (cm^{-1}): 3315-3264 (NH_2), 3153 (N-H, secondary amide), 3055 (C-H, aromatic), 2954, 2839 (C-H, aliphatic), 1670 (C=O, hydrazide), 1606-1573 (C=C, aromatic), 1263-1226 (C-O-C, methoxy), 815 (naphthalene ring out-of-plane bending), with formula: ($C_{14}H_{16}N_2O_2$).

5-(1-(6-methoxynaphthalen-2-yl)ethyl)-1,3,4-oxadiazole-2-thiol (NC) - White solid powder, yield = 90%, m.p. = 192-194 °C. FTIR (cm^{-1}): 3118, 3012 (Aromatic C-

H), 2954, 2904 (Aliphatic C-H), 1631 (C=N, oxadiazole), 1593 (Aromatic C=C), 1459 (CH_3 bending), 1426 (C-H bending, aromatic), 1338 (O-CH3 bending), 1292, 1243 (C-O-C, methoxy), 1119 (C-N, oxadiazole), 1163 (C-S), 661 (S-H), with formula: ($C_{15}H_{14}N_2O_2S$).

New 1-(4-aminophenyl)-2-((5-(1-(6-methoxynaphthalen-2-yl)ethyl)-1,3,4-oxadiazol-2-yl)thio)ethan-1-one (N1) - Crystal solid powder, yield = 65%, m.p. = 172-174 °C. FTIR (cm^{-1}): 3482, 3319 (N-H), 3053 (C-H, aromatic), 2956 (C-H, sp3), 1687 (C=O, ethenone), 1645 (N-H bending), 1595 (C=C, aromatic), 1262 (C-O, methoxy), 1130 (C-S). ^{1}H-NMR; δ 1.37 (Doublet, 3H, CH_3), 3.88 (Singlet, 3H, OCH3), 4.15 (Quartet, 1H, CH), 4.28 (Singlet, 2H, CH), 5.35 (Singlet, 2H, NH_2), 6.78 (Doublet, 2H, CH), 7.02 (Doublet, 1H, CH), 7.11 (Singlet, 1H, CH), 7.46 (Doublet, 1H, CH), 7.70 (Doublet, 1H, CH), 7.74 (Doublet, 1H, CH), 7.78 (Doublet, 2H, CH), 7.90 (Singlet, 1H, CH). ^{13}C-NMR; δ 15.58 (Aliphatic CH_3), 38.80 (CH), 44.55 (Aliphatic CH_2), 55.51 (CH_3 of methoxy), 106.12-157.21 (Aromatic carbons), 164.48-169.53 (Carbons of ring C), 193.79 (Carbonyl group), with formula: ($C_{23}H_{21}N_3O_3S$).

New 1-(4-(dimethylamino)phenyl)-2-((5-(1-(6-methoxynaphthalen-2-yl)ethyl)-1,3,4-oxadiazol-2-yl)thio)ethan-1-one (N2) - Yellow to orange powder, yield = 70%, m.p. = 186-188 °C. FTIR (cm^{-1}): 3112, 3012 (Aromatic C-H), 2971, 2900 (Aliphatic C-H), 1678 (C=O, carbonyl), 1593 (Aromatic C=C), 1546 (N-H bending), 1311 (C-O-C, methoxy), 1230-1165 (C-N), 1122 (C-N), 813 (Aromatic C-H bending). ^{1}H-NMR; δ 1.35 (Doublet, 3H, CH3), 2.93 (Singlet, 6H, CH3), 3.75 (Singlet, 3H, OCH_3), 4.33 (Quartet, 1H, CH), 4.52 (Singlet, 2H, CH_2), 6.77 (Doublet, 4H, CH), 7.03 (Doublet, 1H, CH), 7.22 (Singlet, 1H, CH), 7.46 (Doublet, 1H, CH), 7.72 (Doublet, 1H, CH), 7.78 (Doublet, 1H, CH), 7.80 (Singlet, 1H, CH), 7.81 (Doublet, 4H, CH). ^{13}C-NMR; δ 19.49 (Aliphatic CH_3), 35.46 (CH), 37.69 (Aliphatic CH_2), 44.53 (Dimethyl amine carbons), 52.18 (CH_3 of methoxy), 106.10-158.24 (Aromatic carbons), 163.16-169.21 (Carbons of ring C), 195.42 (Carbonyl group), with formula: ($C_{25}H_{25}N_3O_3S$).

New 2-((5-(1-(6-methoxynaphthalen-2-yl)ethyl)-1,3,4-oxadiazol-2-yl)thio)-1-phenylethan-1-one (N3) - Yellow powder, yield = 75%, m.p. = 174-176 °C. FTIR (cm^{-1}): 3035 (Aromatic C-H), 2911, 2854 (Alkyl C-H), 1702 (C=O, ketone), 1627, 1607 (Aromatic C=C), 1468, 1460 (CH_3 bending), 1298 (C-N, oxadiazole), 1178 (C-O-C, methoxy), 694 (Thiol group). ^{1}H-NMR; δ 1.88 (Doublet, 3H, CH_3), 3.80 (Singlet, 3H, OCH_3), 4.14 (Quartet, 1H, CH), 4.47 (Singlet, 2H, CH_2), 7.01 (Doublet, 1H, CH), 7.18 (Singlet, 1H, CH), 7.49 (Doublet, 1H, CH), 7.54 (Multiplate, 4H, CH), 7.61 (Triplet, 1H, CH), 7.73 (Doublet, 1H, CH), 7.76 (Doublet, 1H, CH), 7.90 (Singlet, 1H, CH), 7.98 (Doublet, 4H, CH). ^{13}C-NMR; δ 17.63 (Aliphatic CH_3), 35.16 (CH), 43.91 (Aliphatic CH_2), 53.65 (CH_3 of methoxy), 106.14-156.50 (Aromatic carbons), 164.04-165.46 (Carbons of ring C), 196.50 (Carbonyl group), with formula: ($C_{23}H_{20}N_2O_3S$).

New 2-((5-(1-(6-methoxynaphthalen-2-yl)ethyl)-1,3,4-oxadiazol-2-yl)thio)-1-(p-tolyl)ethan-1-one (N4) - Off-white to pale yellow crystalline solid, yield = 80%, m.p. = 116-118 °C. FTIR (cm^{-1}): 3053 (Aromatic C-H), 2953, 2899, 2835 (Aliphatic C-H), 1730 (C=O, carbonyl), 1690 (Aromatic C=C), 1598 (Aromatic C=C), 1457, 1411, 1361 (C-H bending), 1260 (C-O-C, methoxy), 1223, 1158 (C-N), 1025 (C-S), 956, 893, 845 (Aromatic C-H out-of-plane bending). ^{1}H-NMR; δ 1.60 (Doublet, 3H, CH_3), 2.47 (Singlet, 3H, CH3), 3.82 (Singlet, 3H, OCH3), 4.41 (Quartet, 1H, CH), 4.51 (Singlet, 2H, CH_2), 7.07 (Doublet, 1H, CH), 7.22 (Singlet, 1H, CH), 7.31 (Doublet, 4H, CH), 7.47 (Doublet, 1H, CH), 7.71 (Doublet, 4H, CH), 7.76 (Doublet, 1H, CH), 7.79 (Doublet, 1H, CH),

7.82 (Singlet, 1H, CH). ^{13}C-NMR; δ 16.33 (Aliphatic CH_3), 21.32 (CH_3 of ring D), 29.50 (CH), 44.54 (Aliphatic CH_2), 55.75 (CH_3 of methoxy), 106.14-157.00 (Aromatic carbons), 164.46-168.34 (Carbons of ring C), 193.95 (Carbonyl group), with formula: ($C_{24}H_{22}N_2O_3S$).

New 1-(4-ethylphenyl)-2-((5-(1-(6-methoxynaphthalen-2-yl)ethyl)-1,3,4-oxadiazol-2-yl)thio)ethan-1-one (N5) - White to off-white crystalline solid, yield = 75%, m.p. = 139-141 °C. FTIR (cm^{-1}): 3107, 3061 (Aromatic C-H), 2964, 2920 (Aliphatic C-H), 1708 (C=O, ketone), 1595 (C=C, aromatic), 1535 (C=N, oxadiazole), 1483 (C-H bending), 1435 (Aromatic C=C and C-H bending), 1315 (C-O-C, methoxy), 1178-1074 (C-S), 1120 (C-N, oxadiazole), 815 (Aromatic C-H out-of-plane bending). ^{1}H-NMR; δ 1.42 (Triplet, 3H, CH_3), 1.62 (Doublet, 3H, CH_3), 2.66 (Quartet, 2H, CH_2), 3.84 (Singlet, 3H, OCH3), 4.45 (Quartet, 1H, CH), 4.66 (Singlet, 2H, CH_2), 7.13 (Doublet, 1H, CH), 7.16 (Singlet, 1H, CH), 7.29 (Doublet, 4H, CH), 7.35 (Doublet, 1H, CH), 7.69 (Doublet, 4H, CH), 7.74 (Doublet, 1H, CH), 7.81 (Doublet, 1H, CH), 7.87 (Singlet, 1H, CH). ^{13}C-NMR; δ 15.57 (CH_3 of ethyl), 19.77 (Aliphatic CH_3), 29.49 (Aliphatic CH_2), 29.53 (CH), 36.41 (Aliphatic CH_2), 55.73 (CH_3 of methoxy), 106.54-165.99 (Aromatic carbons), 164.35-170.46 (Carbons of ring C), 192.23 (Carbonyl group), with formula: ($C_{25}H_{24}N_2O_3S$).

New 2-((5-(1-(6-methoxynaphthalen-2-yl)ethyl)-1,3,4-oxadiazol-2-yl)thio)-1-(4-nitrophenyl)ethan-1-one (N6) - Light yellow to pale yellow crystalline solid, yield = 65%, m.p. = 162-164 °C. FTIR (cm^{-1}): 3053 (Aromatic C-H), 2956, 2934, 2902, 2836 (Aliphatic C-H), 1692 (C=O, ketone), 1605, 1580, 1485 (C=C, aromatic), 1533 (N-O, nitro), 1342 (N-O, nitro), 1306 (C-O-C, methoxy), 1242 (C-O, methoxy), 1174-1072 (C-S), 1217 (C-N, oxadiazole), 815 (Aromatic C-H out-of-plane bending). ^{1}H-NMR; δ 1.73 (Doublet, 3H, CH3), 3.85 (Singlet, 3H, OCH3), 4.33 (Quartet, 1H, CH), 4.40 (Singlet, 1H, CH_2), 6.98 (Doublet, 1H, CH), 7.19 (Singlet, 1H, CH), 7.39 (Doublet, 1H, CH), 7.75 (Doublet, 1H, CH), 7.78 (Doublet, 1H, CH), 7.93 (Singlet, 1H, CH), 8.12 (Doublet, 4H, CH), 8.28 (Doublet, 4H, CH). ^{13}C-NMR; δ 18.62 (Aliphatic CH_3), 35.15 (CH), 38.80 (Aliphatic CH_2), 55.73 (CH_3 of methoxy), 106.11-157.18 (Aromatic carbons), 164.50-167.44 (Carbons of ring C), 190.27 (Carbonyl group), with formula: ($C_{23}H_{19}N_3O_5S$).

New 1-(4-hydroxyphenyl)-2-((5-(1-(6-methoxynaphthalen-2-yl)ethyl)-1,3,4-oxadiazol-2-yl)thio)ethan-1-one (N7) - Brown solid, yield = 80%, m.p. = 152-154 °C. FTIR (cm^{-1}): 3402 (O-H), 3315, 3078 (Aromatic C-H), 2976 (Aliphatic C-H), 1684 (C=O, ketone), 1602 (C=C, aromatic), 1515 (C=C, aromatic), 1467 (C-H bending), 1441 (Aromatic C=C and C-H bending), 1326 (C-O, methoxy), 1207 (C-O, phenolic), 1122-1080 (C-S), 846 (Aromatic C-H out-of-plane bending). ^{1}H-NMR; δ 1.39 (Doublet, 3H, CH3), 3.82 (Singlet, 3H, OCH3), 4.36 (Quartet, 1H, CH), 4.44 (Singlet, 2H, CH_2), 7.00 (Doublet, 4H, CH), 7.10 (Doublet, 1H, CH), 7.23 (Singlet, 1H, CH), 7.32 (Doublet, 1H, CH), 7.67 (Doublet, 1H, CH), 7.77 (Doublet, 1H, CH), 7.80 (Doublet, 4H, CH), 7.85 (Singlet, 1H, CH), 10.19 (Singlet, 1H, OH). ^{13}C-NMR; δ 21.23 (Aliphatic CH_3), 35.42 (CH), 38.80 (Aliphatic CH_2), 55.35 (CH_3 of methoxy), 105.77-161.25 (Aromatic carbons), 164.35-168.70 (Carbons of ring C), 192.79 (Carbonyl group), with formula: ($C_{23}H_{20}N_2O_4S$).

New 1-(4-chlorophenyl)-2-((5-(1-(6-methoxynaphthalen-2-yl)ethyl)-1,3,4-oxadiazol-2-yl)thio)ethan-1-one (N8) - White crystalline solid, yield = 75%, m.p. = 145-147 °C. FTIR (cm^{-1}): 3072, 2891 (Aromatic C-H), 1703 (C=O, carbonyl), 1631 (C=N, oxadiazole), 1585 (C=C, aromatic), 1489 (C=C, aromatic), 1282 (C-O-C, ether), 1068 (C-O, oxadiazole), 844

(Aromatic C-H out-of-plane bending), 758 (C-Cl), 659 (C-S). ^{1}H-NMR; δ 1.90 (Doublet, 3H, CH_3), 3.87 (Singlet, 3H, OCH_3), 4.34 (Quartet, 1H, CH), 4.47 (Doublet, 2H, CH), 7.10 (Doublet, 1H, CH), 7.21 (Singlet, 1H, CH), 7.32 (Doublet, 1H, CH), 7.52 (Doublet, 4H, CH), 7.70 (Doublet, 1H, CH), 7.79 (Doublet, 1H, CH), 7.87 (Singlet, 1H, CH), 7.94 (Doublet, 4H, CH). ^{13}C-NMR; δ 16.22 (Aliphatic CH_3), 35.43 (CH), 36.45 (Aliphatic CH_2), 50.95 (CH_3 of methoxy), 105.56-154.52 (Aromatic carbons), 164.79-169.32 (Carbons of ring C), 197.55 (Carbonyl group), with formula: ($C_{23}H_{19}ClN_2O_3S$).

New 1-(4-bromophenyl)-2-((5-(1-(6-methoxynaphthalen-2-yl)ethyl)-1,3,4-oxadiazol-2-yl)thio)ethan-1-one (N9) - White to off-white crystalline solid, yield = 75%, m.p. = 151-153 °C. FTIR (cm^{-1}): 3053, 2953 (Aromatic C-H), 1705 (C=O, carbonyl), 1631 (C=N, oxadiazole), 1586 (C=C, aromatic), 1483 (C=C, aromatic), 1263 (C-O-C, ether), 1082 (C-O, oxadiazole), 844 (Aromatic C-H out-of-plane bending), 665 (C-S), 550 (C-Br). 1H-NMR; δ 1.81 (Doublet, 3H, CH3), 3.89 (Singlet, 3H, OCH3), 4.16 (Quartet, ^{1}H, CH), 4.45 (Doublet, 2H, CH), 7.15 (Doublet, 1H, CH), 7.20 (Singlet, 1H, CH), 7.50 (Doublet, 1H, CH), 7.68 (Doublet, 4H, CH), 7.73 (Doublet, 1H, CH), 7.81 (Doublet, 1H, CH), 7.89 (Singlet, 1H, CH), 7.96 (Doublet, 4H, CH). ^{13}C-NMR; δ 17.98 (Aliphatic CH3), 34.33 (CH), 46.64 (Aliphatic CH2), 54.21 (CH3 of methoxy), 106.52-158.48 (Aromatic carbons), 164.45-168.37 (Carbons of ring C), 191.33 (Carbonyl group), with formula: ($C_{23}H_{19}BrN_2O_3S$).

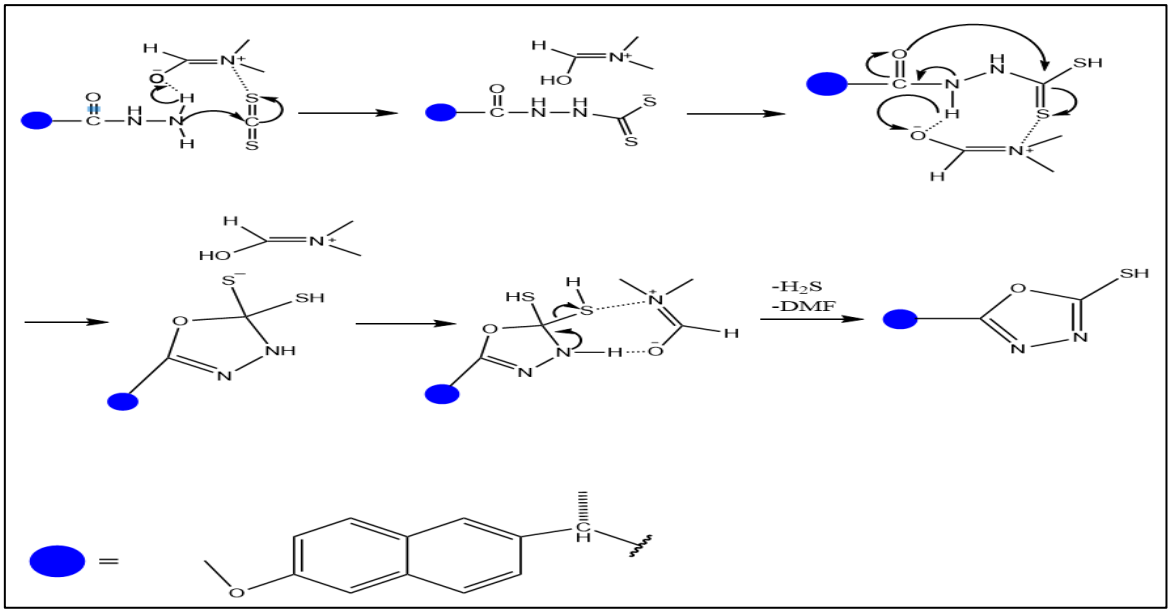

Scheme (2): Mechanism of Compound (NC) (2-Mercapto oxadiazole of S-Naproxen) [10].

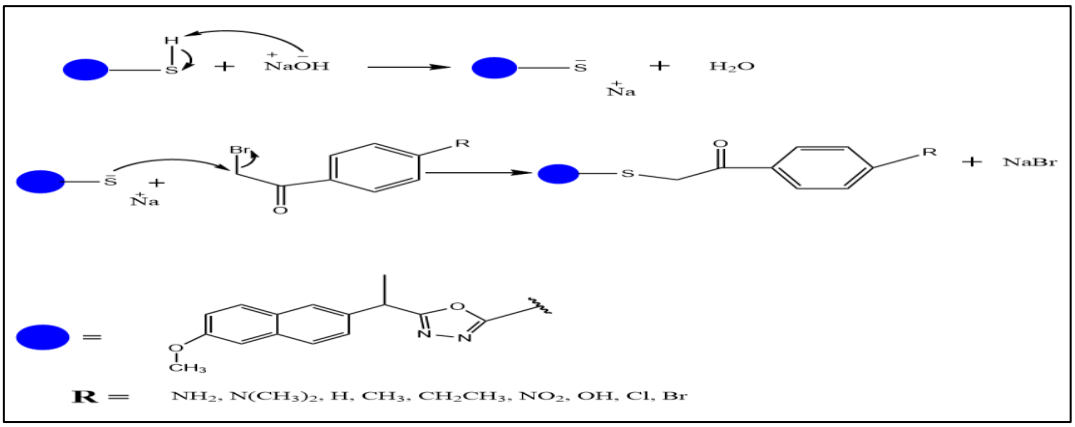

Scheme (3): Mechanism of final compounds [11].

Cytotoxic Activity against A549 Lung Cancer Cells results

The synthesized compounds N1–N9 were subjected to preliminary cytotoxicity screening against A549 human lung cancer cells using the MTT assay. This cell line was chosen as a representative NSCLC model that is known to be EGFR-expressing and is widely used in anticancer drug evaluation. Osimertinib, an EGFR inhibitor, was used as a reference drug to benchmark the activity of our compounds. The antiproliferative effects were assessed at 24, 48, and 72 hours of treatment, and dose–response curves were generated to calculate IC_{50} values at each time point.

The results (Table 1) show that all nine naproxen-oxadiazole derivatives exhibited considerable growth inhibition of A549 cells, with IC_{50} values ranging roughly from 3 to 10 µg/mL (which corresponds to approximately 6–20 µg/Ml) at 72 hours. In general, longer exposure (48–72 h) led to enhanced cytotoxic effects (lower IC_{50}) for most compounds, indicating time-dependent antiproliferative activity. A comparison with Osimertinib revealed that several of investigated compounds were of comparable or greater potency under the experimental conditions. For instance, compound N6 (4-nitrophenyl substituent) was exceptionally active at 24 h, with an IC_{50} of 2.94 µg/mL, markedly more potent than Osimertinib's IC_{50} of 5.31 µg/mL at 24 h . This suggests a rapid cytotoxic action by N6. However, interestingly, N6's potency did not further improve at 72 h (IC_{50} drifted to 4.70 µg/mL) , which might indicate some reversal effect or reduced stability/availability of N6 over time. In contrast, other compounds showed their best performance at the 72h mark. Notably, compound N9 (4-bromophenyl) emerged as the most potent derivative after 72 h, with IC_{50} = 2.95 µg/mL, slightly better than the Osimertinib IC_{50} = 3.10 µg/mL at 72 h . Compound N7 (4-hydroxyphenyl) was similarly effective (IC50 3.00 µg/mL at 72 h) , outperforming Osimertinib at that time point. Compounds N4 (4-methylphenyl) and N3 (unsubstituted phenyl) were relatively less potent, with 72 h IC_{50} values of 5.10 and 6.30 µg/mL, respectively . These were still in the micromolar range, but about 1.5–2 times higher than Osimertinib's efficacy. The remaining derivatives fell in between: N1 (4-aminophenyl) and N5 (4-ethylphenyl) both achieved 3.2–3.3 µg/mL IC_{50} at 72 h (virtually equivalent to Osimertinib) , while N2 (4-(dimethylamine) phenyl) and N8 (4-chlorophenyl) had IC_{50} around 4 µg/mL at 72 h . It is worth noting that N8 (para-choro) showed an IC_{50} of 3.10 µg/mL at 72 h , effectively matching Osimertinib. The slight differences in activity among compounds can be attributed to the electronic and hydrophobic nature of the substituents, which may affect cell permeability, target binding, or other pharmacodynamic/pharmacokinetic properties.

Table (1): IC_{50} of the synthesized compounds and Osimertinib for three-point times

Compound	IC_{50} 24h	IC_{50} 48h	IC_{50} 72h
N1	9.63	8.30	3.30
N2	7.99	7.41	4.20
N3	6.99	3.38	6.30
N4	3.67	3.18	5.10
N5	3.67	3.19	3.20
N6	2.94	3.98	4.70
N7	9.00	5.41	3.00
N8	7.01	4.81	3.10
N9	7.81	3.89	2.95
Osimertinib	5.31	2.13	3.10

To better visualize the structure–activity relationship (SAR) trends, we consider the substituent effects: The most potent compounds at 72 h, N7 (4-OH) and N9 (4-Br), contain substituents that are moderately electron-donating (hydroxyl can donate via resonance) or electron-withdrawing (bromine is weakly withdrawing and adds hydrophobic bulk). Both –OH and –Br are capable of engaging in specific interactions (hydrogen bonding for –OH, and halogen bonding or enhanced hydrophobic contacts for –Br) in a biological context, which might contribute to higher activity. N8 (4-Cl) is similar to N9 and indeed showed comparable activity. On the other hand, N3 (phenyl with no substituent) was the least active, suggesting that having a substituent at the para position is beneficial. The strongly electron-donating N2 (4-$N(CH_3)_2$) and strongly electron-withdrawing N6 (4-NO_2) showed good initial potency but did not significantly improve over time or reach the lowest IC_{50}, perhaps indicating that extreme electronic effects are not optimal for sustained activity. A possible explanation is that very polar substituents (like –NO_2 or –NMe_2) might affect cellular uptake or compound stability. N1 (4-NH_2) was quite active and improved from 9.6 µg/mL at 24 h to 3.3 µg/mL at 72 h , which could be due to the formation of intracellular interactions (the free –NH2 may allow formation of conjugates or enhanced binding to targets over time). N4 (4-CH_3) and N5 (4-C_2H_5) both have alkyl groups; N5 with an ethyl was more potent (IC_{50} 3.2) than N4 with a methyl (5.1 µg/mL), hinting that a slightly bulkier/aromatic substituent is preferable to a small one. Overall, while all compounds share the same core, the para substituent on the phenacyl phenyl ring modulates activity, with a trend that para-hydroxyl and halogens confer strong activity, whereas an unsubstituted or small substituent is less favorable. This SAR insight could be valuable for future optimization (for example, 4-OCH_3 or 4-CF_3 substituents could be explored as they might combine electronic and lipophilic properties).

Importantly, when comparing to Osimertinib, our compounds performed remarkably well given that Osimertinib is a potent targeted agent. At 24 h, Osimertinib's IC_{50} in our assay was 5.31 µg/mL (which is roughly 10 µg/mL, consistent with its known sub- µg/mL potency in EGFR mutant lines but higher in EGFR wild-type A549 cells). By 72 h it was 3.10 µg/mL . Several of the naproxen-oxadiazole derivatives equaled or exceeded this potency, which is highly encouraging. For example, N9 (4-Br) showed slightly better efficacy at all time points (7.81 vs 5.31 at 24 h, 3.89 vs 2.13 at 48 h, and 2.95 vs 3.10 µg/mL at 72 h, comparing N9 to Osimertinib) . Although Osimertinib was more potent at 48 h, N9 caught up by 72 h. Similarly, N7 (4-OH) had 72 h IC_{50} 3.0 µg/mL, edging out Osimertinib . N5 (4-ethyl) and N8 (4-chloro) were virtually equipotent to Osimertinib at 72 h (3.20 and 3.10 µg/mL, respectively) . On the other

hand, N3 and N4 were weaker, indicating room for improvement in those analogues. Nonetheless, the overall strong activity of this series suggests that the design strategy linking a pharmacologically active naproxen fragment with a heterocyclic oxadiazole-thioether moiety – has yielded compounds with inherent anticancer properties.

The mechanism of action of these compounds at the molecular level remains to be elucidated. We hypothesize they are, analogous to the reference drug Osimertinib and the literature examples are cited earlier, these naproxen-oxadiazole derivatives may act as kinase inhibitors, potentially targeting EGFR or other tyrosine kinases involved in A549 cell survival. The presence of the 1,3,4-oxadiazole and the 2-methoxynaphthalene (naproxen) moiety in one molecule creates a scaffold that could bind to the ATP site of kinases [14]. The varied para-substituents might interact with different pockets in a kinase active site (for example, a para-halogen could occupy a hydrophobic sub-pocket, whereas a para-OH could form hydrogen bonds). These is hypothesis warrant further investigation such as enzyme inhibition assays or molecular docking (which was performed in the thesis work but is beyond the scope of this article) would be needed to confirm the targets. It is also plausible that these compounds induce apoptosis or cell cycle arrest through COX-2 inhibition or other pathways, considering the naproxen portion. However, A549 is not primarily driven by COX-2, and the rapid effects observed (24 h IC_{50} in low micromolar range) favor a direct cytotoxic or anti-proliferative mechanism rather than a classical NSAID effect [15].

Another point of interest is the selectivity and toxicity profile. In this preliminary assay, the synthesized compounds were only tested against a cancer cell line. It would be important to evaluate the compounds against normal (non-cancerous) cells to gauge selectivity. The use of a normal fibroblast cell line (HdFn) for testing similar compounds was reported in the thesis the literature (as flavopiridol was compared in the example article) [16]. While we have not yet performed such tests, ideally the goal is to find compounds that are more toxic to cancer cells than to normal cells. NSAIDs like naproxen have some degree of safety in normal tissues, and if that property carries over in these derivatives, it could be beneficial [17]. The structural features (e.g., polar groups like –OH, $–NH_2$) might also influence solubility and distribution, which in turn affect toxicity. Further ADME studies and broader biological evaluations (e.g., testing on additional cancer cell lines, kinase panel screening) would be warranted to fully establish the pharmacological profile of N1–N9.

In summary, the cytotoxicity results demonstrate that the novel S-naproxen 1,3,4-oxadiazole thioether compounds possess significant anti-lung cancer activity in vitro. Several compounds in the series are comparable to the established EGFR inhibitor Osimertinib against A549 cells, highlighting the success of our design strategy. The presence of different aromatic substituents allowed us to identify favorable features (such as 4-OH and 4-halogen) for activity [18]. These findings validate the concept of integrating an NSAID scaffold with a heterocyclic moiety to yield potential anticancer agents [19]. The encouraging in vitro efficacy of compounds like N7, N8, and N9 suggests they could serve as lead compounds for further development. Future work will focus on delineating their mechanism of action (e.g., kinase inhibition assays) and optimizing their properties (for instance, modifying substituents or improving solubility) to advance these compounds toward preclinical candidacy.

Conclusions

In this study, a series of target compounds were successfully synthesized, a series of novel 1,3,4-oxadiazole thioether derivatives of S-naproxen and demonstrated their potential as anticancer agents against lung

cancer cells. The synthetic route, involving esterification, hydrazide formation, cyclization to 1,3,4-oxadiazole-2-thiol, and S-alkylation, provided nine final compounds (N1–N9) in good yields and high purity. Comprehensive structural characterization (FT-IR, $^{1}H/^{13}C$-NMR, melting point, TLC) confirmed that the targeted structures were obtained. Notably, key spectral features such as the emergence and disappearance of functional group signals at each step were consistent with the expected chemical transformations, underscoring the success of the synthetic strategy.

Biological evaluation using the MTT assay revealed that all the synthesized compounds possess cytotoxic activity against the A549 human lung cancer cell line. The IC_{50} values were in the low micromolar range, and several derivatives (especially those with para-substituents like –OH, –Br, –Cl, –NH_2) showed potency comparable to or exceeding that of Osimertinib, a current targeted therapy for NSCLC. For example, compound N9 (4-Br) achieved an IC_{50} of 2.95 µg/mL at 72 h, slightly better than Osimertinib under the same conditions. These results are quite promising for a first-generation analog series and suggest that the naproxen-oxadiazole-thioether scaffold is inherently active against cancer cells. The preliminary SAR indicates that the nature of the para-substituent on the phenyl ring can modulate activity, providing insight for future optimization [20]. The combination of an anti-inflammatory pharmacophore (naproxen) with a versatile heterocycle (1,3,4-oxadiazole) and appropriate aromatic substituents has yielded molecules that interfere with cancer cell viability, potentially through kinase inhibition or related mechanisms. These compounds merit further investigation to fully elucidate their molecular targets and evaluate their therapeutic window. Ongoing and future studies will focus on extending the biological evaluations (including testing on additional cancer models and normal cells), performing mechanistic assays (such as EGFR or VEGFR-2 enzyme inhibition tests), and refining the compound structures for enhanced efficacy and selectivity. The favorable initial results reported here lay a strong foundation for the development of this class of compounds as potential anticancer agents for lung cancer and possibly other malignancies.

References

1- Schneider B, Benzekry S, Mochel J. Comprehensive joint modeling of first-line therapeutics in non-small cell lung cancer. *arXiv* preprint 2401.07719; 2024. doi:10.48550/arXiv.2401.07719

2- Alam MM, Nazreen S, Almalki ASA, *et al.* Naproxen-based 1,3,4-oxadiazole derivatives as EGFR inhibitors: design, synthesis, anticancer and computational studies. *Pharmaceuticals.* 2021;14(9):870. doi:10.3390/ph14090870

3- Deng Y, Ma Y, Ni N, *et al.* Synthesis and biological evaluation of novel 1,3,4-oxadiazole derivatives as potential EGFR tyrosine-kinase inhibitors. *Bioorg Med Chem Lett.* 2015;25(3):579-583. doi: 10.1016/j.bmcl.2014.12.037

4- Kumar D, Patel G, Chittepu VCSR, *et al.* 1,3,4-Oxadiazole derivatives as anticancer agents: a review. *Mini Rev Med Chem.* 2016;16(11):869-885. doi:10.2174/1389557516666160219145313

5- Harris RE. Cyclo-oxygenase-2 (COX-2) and the inflammogenesis of cancer. *Subcell Biochem.* 2007; 42:93-126. doi:10.1007/978-1-4020-5687-1_5

6- Kolawole OR, Kashfi K. NSAIDs and cancer resolution: new paradigms beyond cyclo-oxygenase. *Int J Mol Sci.* 2022;23(3):1432. doi:10.3390/ijms23031432.

7- Hagras M, Saleh MA, Ezz Eldin RR, *et al.* 1,3,4-Oxadiazole–naphthalene hybrids as potential VEGFR-2 inhibitors: design, synthesis,

antiproliferative activity, apoptotic effect and *in-silico* studies. *J Enzyme Inhib Med Chem.* 2022; 37:380-396. doi:10.1080/14756366.2021.2015342

8- Akter M, Al Mahmud Z, Uddin MM, Das R, Rahman SA. Synthesis of naproxen esters and evaluation of their *in-vivo* and *in-silico* analgesic and anti-inflammatory activities. *Dhaka Univ J Pharm Sci.* 2023;22(1):105-114. doi:10.3329/dujps.v22i1.67101

9- Solomons TWG, Fryhle CB. Organic chemistry. 12th ed. 2023;1164.

10- Yarmohammadi E, Beyzaei H, Aryan R, Moradi A. Ultrasound-assisted, low-solvent and acid/base-free synthesis of 5-substituted 1, 3, 4-oxadiazole-2-thiols as potent antimicrobial and antioxidant agents. Molecular Diversity. 2021;25:2367-78. doi:10.1007/s11030-020-10125-y.

11- Hamlin TA, Swart M, Bickelhaupt FM. Nucleophilic substitution (SN2): dependence on nucleophile, leaving group, central atom, substituents, and solvent. ChemPhysChem. 2018 Jun 5;19(11):1315-30, DOI**:** 1002/cphc.201701363.

12- Mirzaei S, Eisvand F, Nejabat M, Ghodsi R, Hadizadeh F. Anticancer Potential of a Synthetic Quinoline, 9IV-c, by Inducing Apoptosis in A549 Cell and In vivo BALB/c Mice Models. Anti-Cancer Agents in Medicinal Chemistry-Anti-Cancer Agents). 2024 Feb 1;24(3):185-92.

13- Pavia DL, Lampman GM, Kriz GS. Introduction to Spectroscopy. 5th ed. Boston: Cengage Learning; 2014.

14- Ge X, Zhang Y, Huang F, *et al.* EGFR tyrosine-kinase inhibitor almonertinib induces apoptosis and autophagy mediated by reactive oxygen species in non-small cell lung cancer cells. *Hum Exp Toxicol.* 2021;40(12 Suppl):S49-S62. doi:10.1177/09603271211030554

15- Mohamed MF, Ahmed EA, Alshazly O, *et al.* Synthesis, anticancer and anti-inflammatory evaluation of novel quinoxaline-1,3,4-oxadiazole derivatives as EGFR and COX-2 inhibitors. *J Mol Struct.* 2025;141651. doi:10.1016/j.molstruc.2025.141651

16- Rahimi S, Chen Y, Zareian M, Pandit S, Mijakovic I. Cellular and subcellular interactions of graphene-based materials with cancerous and non-cancerous cells. *Adv Drug Deliv Rev.* 2022;189:114467. doi:10.1016/j.addr.2022.114467

17- Farah Haidar, Monther Faisal Mahdi, Ayad Kareem Khan. Synthesis, Molecular Docking, Characterization, and Preliminary Evaluation of Some New 1, 3-Diazetidin-2-One Derivatives as Anticancer Agents. (2024). Al Mustansiriyah Journal of Pharmaceutical Sciences, 24(1), 48-58. https://doi.org/10.32947/ajps.v24i1.1026.

18- Zaid Nazar Ibrahim, Ayad Kareem Khan, Mohammed Dheyaa Hamdi, Atheer Awad Mehde. Drug Design, In Silico-Profiling of New Pyrrole Derivatives: Promising Anticancer Agents Against Acute Myeloid Leukemia. (2024). Al Mustansiriyah Journal of Pharmaceutical Sciences, 24(3), 252-263. https://doi.org/10.32947/ajps.v24i3.1063.

19- Ding S, Gao Z, Hu Z, *et al.* Design, synthesis and biological evaluation of novel osimertinib derivatives as reversible EGFR kinase inhibitors. *Eur J Med Chem.* 2022;238:114492. doi:10.1016/j.ejmech.2022.114492.

20- Yasir F. Muhsin, Shakir M. Alwan, Ayad Kareem Khan. Design, Molecular Docking, Synthesis of Aromatic Amino Acids Linked to Cephalexin. (2022). Al Mustansiriyah Journal of Pharmaceutical Sciences, 21(3), 25-34. https://doi.org/10.32947/ajps.v21i3.794.